Vision guided learning based intelligent sewing system

Bidan Huang, Alessandro Vandini, Yang Hu, Guang-Zhong Yang, *Fellow, IEEE*

***Abstract*— This paper presents an intelligent sewing system for personalized stent graft manufacturing. Hand sewing is a challenging task for robotics, as it requires a high level dexterity and accuracy. Inspired by the medical suturing robots, we use a curved needle to achieve the task. We motorize a needle driver and attach it to a 7 d.o.f robot arm to manipulate the needle. Learning from demonstration approach is used to program the robot to sew the sent in the fabric. The demonstrated sewing skill is firstly segmented to several phases, and is encoded by statistical models. Robot sewing movements are generated from the models and are used for task execution. During the execution, a stereo vision system is adopted and guide the robot to adjust the learnt movement according to the needle pose. The system is implemented on a real robot system. We presents two experiments with this system and analyse the result experimental quantitatively. We show that our approach can robustly perform sewing with the same quality, as well as adapt to various needle pose.**

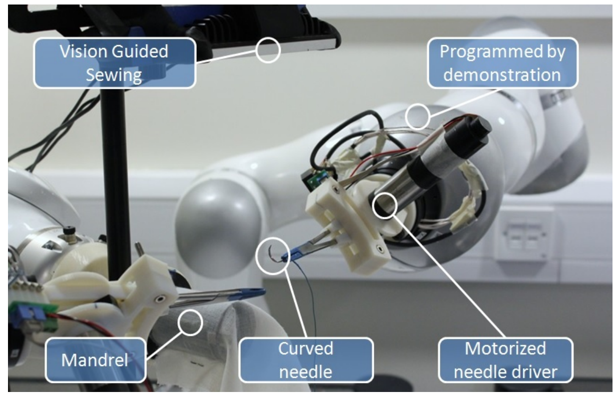

Fig. 1: Robot sewing system for personalized stent graft manufacturing

I. Introduction

Sewing is a delicate and pain-stacking task. Recent development in robotics has largely increased the efficiency of the sewing industry. Most of these robotic solutions are specialised in one or a few certain types of machine stitches, such as the lock stitches. Some conventional hand stitches are hard to automate and still requires human labour. Our motivation of the study is to free human from the tiring sewing jobs and teach the robot to make hand stitches. Particularly, we focus on the task of personalized stent graft manufacturing.

A stent graft is a tubular structure composed of fabric supported by a metal mesh called stent. It is widely used for a variety of pathologies during endovascular interventions, such as reinforcing the vessel wall in presence of aneurysms. Clinically, each stent graft needs to be customised to the patient anatomy, with fenestrations (openings) on the graft body to maintain the patency of side branches to vital organs. They often come at a significant cost in addition to a long manufacturing process. This is mainly due to the intensive manual tasks involved in the process. As a consequence, patients are more likely to be subjected of complications, e.g. aneurysm eruption, during the waiting period and precluding treatment to patients presenting acutely. Improved manufacturing of personalised stent grafts is therefore a critical unmet clinical demand and we are pursuing a robot assisted manufacturing approach. This study focuses on the key process of the stent graft manufacturing: sewing the stent to a fabric tube. For this purpose, a robotic system is proposed here in order to replicate the hand stitches required during the stent graft manufacturing process.

Automated sewing has been extensively researched in textile industry. Intelligent robotic systems with multi-sensor feedback are built to work in conjunction with a traditional sewing machine. Important topics in this filed includes bimanual robotic sewing [7], fabric tension control, and seam tracking [15], [16]. To cope with environmental changes during the sewing process, various control strategies are implemented, such as a fuzzy logic controller [6], a hybrid position/force control [7], a leader/follower control strategy [14]. In addition, extensive research has been carried out in the design of sewing heads capable of access the sewn object from a single side, which allows the sewing to be performed on a 3D surface. For example, KSL Keilmann (Lorsch, Germany) [6] has develop various 3D stitching systems incorporating single sided sewing heads onto KUKA manipulators for sewing fabric-reinforced structure of aircraft parts. These machines are designed for sewing large and heavy objects. Delicate sewing for small objects with non uniform shapes are still mainly hand made.

As the emerging of robotic assisted systems in the field of minimally invasive surgery, research on automated suturing tasks is also widely investigated, which provides the advantage of the machine speed and accuracy of the suturing process. A suturing task can be divided into two sub-tasks: tissue piercing and knot tying. For each task, research is carried by planning the procedure according to well established manual suture techniques [4], [5], [11] or learning the skills from expert demonstrations [10], [12], [18]. Vision guidance/visual servoing plays a key role in the achievement of a fully automated suturing task. In the

B. Huang, A. Vandini, Y. Hu and G.-Z. Yang are with the Hamlyn Centre for Robotic Surgery, Imperial College London, SW7 2AZ, London, UK (e-mail: b.huang@imperial.ac.uk). Bidan Huang and Yang Hu was supported by the EPSRC (EP/L020688/1).

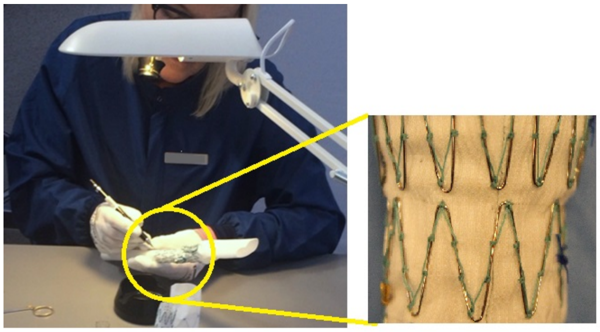

Fig. 2: A lady is hand sewing stent graft.

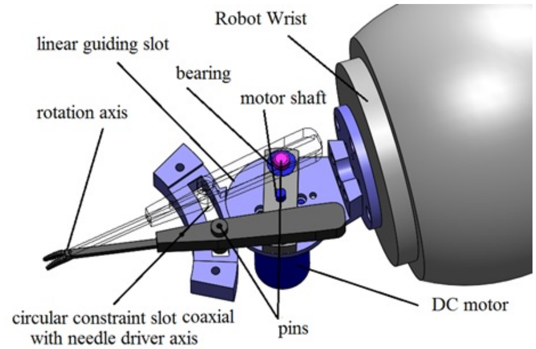

Fig. 3: Motorized needle driver

aspect of positioning the needle to the target point, both the needle posture and the target suturing plane posture need to be measured. Iyer et al. [3] proposed a single arm single camera system auto-suturing system in which the area being sutured on is marked by round markers. In their method, the monocular pose measurement algorithm [9] was used for estimating the needle posture. Another work presented by Staub et al. [17] introduced 3D stereo system and visual servoing technique to improve the accuracy in aligning the needle with target stitching point. Recently, an auto-suturing system with 2D camera guidance and motorized Endo 360 suturing device is presented [8]. In this work, a method is presented to track incision contour and automatically distributes equally-spaced stitches along the incision.

Inspired by these medical sewing approaches, we use robots to control a needle driver to manipulate a curved needle for sewing. Compare to conventional sewing machines, this approach is more versatile, allowing us to do stent sewing, fenestration finishing and knot tying with the same setup. A learning from human demonstration approach is used here so that the robot sewing movements can be programmed easily.

The use of curve needle also gives us the benefit of doing single sided sewing. The shape of the fabric tube, i.e. the graft, is pre-designed for the patient anatomy and pre-manufactured. The tube can not be flattened into a single layer and hence conventional techniques of sewing a flat fabric is not applicable. Single sided sewing is an effective solution. Inspired by the conventional method of sewing stent grafts, we design a mandrel to support the fabric from the inside (Figure 2). Figure 1 shows our sewing system. To ensure the stitch quality and the system robustness, we use a vision system to guide the sewing process. As far as we know, this is the first automotive sewing system that use curved needle to make hand stitches.

This paper presents the proposed system and is organized as follows. Section 2 describe our system, both the hardware design and the software components. Section 3 shows the experiments we conduct using this system and presnets the results, followed by the discussion in Section 4.

II. System Overview

This section describes our system for robot sewing with a curved needle. Our system is consisted with two Kuka 7 d.o.f robots: one robot to manipulate the needle, i.e. piercing and one to control the fabric tube. The robot manipulating the needle is mounted with a motorized needle driver and the one controlling the fabric is mounted with a mandrel. This mandrel is placed inside the fabric tube to bound it tightly with the stent (Figure 4). To ensure the the stent graft quality, each stitch is required to be at the correct place and have the correct length. We use a vision system to guide the robot movements in order to maintain the accuracy. The needle position is tracked during the whole task. The robot movements are first learned from human hand stitch demonstrations and then regenerated online to deliver the needle to stitch at the correct spot.

A. *Hardware design*

A surgical curved needle is used in our task to perform sewing (Figure 1). It is manipulated by a surgical needle driver. This needle driver is widely used in laparoscopic surgery and is specially designed to hold firmly the needle. In our system, the needle driver is motorized for the robot to drive it (Figure 3). This design has two set of constraints/guiding slots working in conjunction with pins. The linear slot lies in the direction along the handle of the needle driver and the constraint slot is coaxial with the needle driver axis; therefore the motor rotation can be mapped to the open and close of the needle driver. To reduce frictions in driving this mechanism, bears are used. All the mechanical components are 3D printed.

Our mandrel is a 3D printed hollow cylinder to support the fabric. Its outer surface has groove for fixing stent and it supports the stent to tightly attache with the fabric. Slots are opened on the mandrel at the positions of stitches. They allow the needle to pierce in and out and hence sewing the stent on the fabric. An additional function of the slots is location marker: when illuminated from inside the mandrel, the location of the slots are visible, allowing us to identify the exact sewing positions.

B. *Learning from human demonstration*

With the current state of art, personalized stent grafts are hand sewn. This is because the delicate control of the needle is hard to programm to robotize. To tackle this problem, we adopt an learning for human demonstration approach

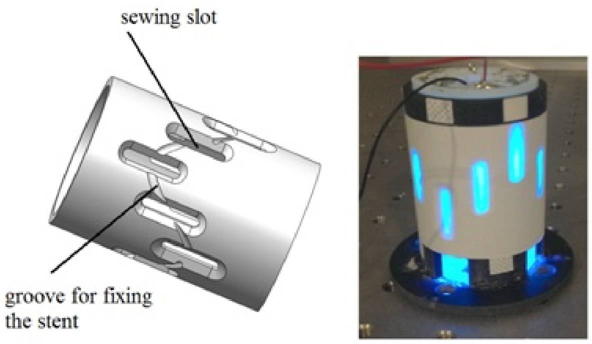

Fig. 4: Mandrel

for this task. Our learning starts by demonstrating to the robot multiple times how to make a stitch. The demonstrated motions are then segmented to different phases. A Gaussian Mixture Model (GMM) [2] is used to encode each phases of the sewing motion and the generalised motion is then retrieved via Gaussian Mixture Regression (GMR). Generally speaking, this learning process involves the following steps:

1) 1: Human demonstration of sewing
2) 2: Motion segmentation
3) 3: Primitive motions learning

1) Human demonstration of sewing: The first step is to recode the stitching motion from human demonstrations. Human single side hand sewing motion involves a couple of stages including 1) needle approaching fabric, 2) needle piercing in, 3) releasing needle end 4)griping the needle tip and 5) pulling the needle out, 6) passing the needle to another hand and 7) picking up the needle head. At the beginning of the task, the needle driver grip firming the needle end. When the tip of the curved needle pierces out from the bottom of the fabric, the needle driver release the needle. The needle is remained in the same pose by the friction of the fabric. The needle driver is then approach the tip of the needle, and grip the tip. The needle then being pulled out from the fabric. Once the needle is completely pulled out from the fabric, the needle driver pass it to another fixed needle driver to re-grip the needle head. After re-griping, the needle driver move back to the starting position and finish a full circle of one stitch.

We use the kinesthetic teaching method to demonstrate all these stages to the robot. The robot is put in gravity compensation mode and its movement is guided by human. The needle driver open and close is controlled an electronic footpedal. The movement of the robot, as well as the needle driver status, i.e. open and close, are recorded. During the demonstrations, when the needle driver is close, we assume the needle is firmly connected with the driver and hence no slip between the needle and the driver will occur. Hence, during the demonstrations, we presume the relative pose between the needle and the driver is a constant value. At the beginning of each demonstration, we place the needle in an optimal pose relative to the needle driver, such that the needle position can be easily computed from the end effector position. All the trajectories are recorded in 6 d.o.f with euler angles $\{\alpha,\beta,\theta\}$ representation of the orientation and $\{x,y,z\}$ representing the robot end effector position.

During the needle driver is griping the needle, we take an object centric approach of learning. This is to say, we learn the motion of the object, i.e. the needle, rather than the movement of the robot. This object centric approach allow us to generate adaptive robot motions to perform the same stitch under different conditions, such as different needle poses. In our task, the needle movements for each stitch should the exactly the same so that the quality of the sewing is maintained. When the robot release the needle, we learn the robot movements so that it approaches the needle tip in a proper pose to grip it. To this end, we segment the stitch motions to different phases. The next section details our segmentation method.

2) Motion segmentation: With all the collected training data (sewing trajectories), we segment each trajectory to reflect the different phases of sewing and learn each phases independently. This segmentation is done based on the relation between the needle and its driver: attached or detached. When the needle is attached to the driver, we take the object centric approach and learn the needle movement so that the needle can repeat the same movement every time. When the needle is detach to the driver, we focus on learning the needle driver trajectory in order to reach the proper location to grip the needle.

Therefore, we use the needle driver open and close events to segment the trajectories (Figure 6). Each segment is then learned as a primitive movement and encoded by a statistical model.

Before learning models for each primitive movements, we apply the Dynamic Time Warping (DTW) [1] to align the data across different demonstrations. DTW is a technique that temporally warps the data and find the best match between two time series according to their key features. In our task, velocity variations do not effect the task quality and hence DTW does not effect our training data.

3) Primitive motion learning: After the we segments the data to a set of primitive movements, we build a model *Omega* to encode each primitive. The same primitive of different trails of the demonstrations are put together as the training data. Each primitive is represented in seven dimension: one temporal value $\{t\}$, three spatial values $h=\{x,y,z\}$ and three orientation values $o=\{\alpha,\beta,\theta\}$. A joint distribution $p\{t,h,o \mid \Omega\}$ is builded by using *GMM*. We choose to use *GMM* because of it's capability of encoding non-linear data and it's robustness of extracting constrains from noise data.

With N Gaussian components, the joint distribution is represented as:

$$
\begin{aligned}
p(t,h,o \mid \Omega) &= \sum_{n=1}^{N} \pi_n p(t,h,o \mid \mu_n, \Sigma_n) \\
&= \sum_{n=1}^{N} \pi_n \frac{1}{\sqrt{(2\pi)^D \mid \Sigma_n \mid}} e^{-\frac{1}{2}(\{t,h,o\}-\mu_n)^\top \Sigma_n^{-1}(\{t,h,o\}-\mu_n)}
\end{aligned} \tag{1}
$$

where π_n is the prior of the n^{th} Gaussian component, D the number of variables, and the μ_n, Σ_n the corresponding mean and covariance. For the n^{th} Gaussian component, the mean and covariance μ_n, Σ_n is:

$$
\boldsymbol{\mu}_n = \begin{pmatrix} \boldsymbol{\mu}_{t,n} \\ \boldsymbol{\mu}_{h,n} \\ \boldsymbol{\mu}_{o,n} \end{pmatrix} \qquad \boldsymbol{\Sigma}_n = \begin{pmatrix} \boldsymbol{\Sigma}_{tt,n} & \boldsymbol{\Sigma}_{th,n} & \boldsymbol{\Sigma}_{to,n} \\ \boldsymbol{\Sigma}_{ht,n} & \boldsymbol{\Sigma}_{hh,n} & \boldsymbol{\Sigma}_{ho,n} \\ \boldsymbol{\Sigma}_{ot,n} & \boldsymbol{\Sigma}_{oh,n} & \boldsymbol{\Sigma}_{oo,n} \end{pmatrix} \tag{2}
$$

Each primitive movement is encoded by one model. A smooth generalized trajectory satisfying the constraints encoded with the *GMM* is extracted by using the Gaussian Mixture Regression (GMR). With the $i-th$ primitive movement model Ω_i, we use a temporal value t to query the trajectory $\{h,o\}$. Here we define:

$$
\mu_n = \begin{pmatrix} \mu_n^t \\ \mu_n^{ho} \end{pmatrix} \qquad \Sigma_n = \begin{pmatrix} \Sigma_n^{tt} & \Sigma_n^{t,ho} \\ \Sigma_n^{ho,t} & \Sigma_n^{ho,ho} \end{pmatrix} \tag{3}
$$

The *GMR* estimate the conditional expectation value as $\hat{\mu}_{ho}$ with variance $\hat{\Sigma}_{ho}$:

$$
\hat{\mu}^{ho} = \sum_{n=1}^{N} \beta_n \hat{\mu}_n \qquad \hat{\Sigma}^{ho,ho} = \sum_{n=1}^{N} {\beta_n}^2 \hat{\Sigma}_n \tag{4}
$$

where

$$
\hat{\mu}_n = \mu_n^{ho} + \Sigma_n^{ho,t} (\Sigma_n^{tt})^{-1} (t - \mu_n^{ho}) \tag{5}
$$

$$
\hat{\Sigma}_n = \Sigma_n^{ho,ho} - \Sigma_n^{ho,t} (\Sigma_n^{tt})^{-1} \Sigma_n^{t,ho} \tag{6}
$$

and

$$
\beta_n = \frac{\pi_n p(t|\mu_n^t, \Sigma_n^{tt})}{\sum_{n=1}^{N} \pi_n p(t|\mu_n^t, \Sigma_n^{tt})} \tag{7}
$$

C. Vision System

The vision system is a key part to maintain the our stitch quality. During the sewing task, defect can occur by the slippage of the needle on the needle drivers. This usually happens during the passing stage: when one needle driver passes the needle to another, small displacements of the optimal relative pose between the needle and the needle driver can occur. The robot movements hence need to adapt to this displacement and generate a new movement to delivery the needle. We use a stereo vision system to monitor the process and measure the displacements. Adaptive robot movements are then generated accordingly. In this section, we explain the method we use for detecting the needle pose.

First, the needle is detected in each stereo image using the needle detection algorithm proposed in [13]. For this purpose, a feature image, i.e. I_H, based on the analysis of the eigenvalues of the Hessian matrix [19] is computed to enhance curvilinear structure in the image. Assuming that a calibrated imaging system is available, the 3D points of the needle defined by its optimum pose are projected in the image plane. This is performed in order to include a prior information of needle's shape in the detection algorithm. Although the optimum pose of the needle is usually different from its real one due to slippage, it still represents of a good guess of the needle pose. Thus, small straight segments are detected in I_H, and only segments that are close to the projected needle and have similar orientation are considered as needle's parts. Finally, these segments are combined in order to create a continuous curve that represents the detected needle in the images. To improve the detection of the needle, the needle driver is also detected in the images using color-base segmentation in HSV space. This allows the reduction of false positive detections of needle segments which are mainly caused by the presence of the needle driver.

The 3D reconstruction of the needle is performed by triangulating the detected needle points of the stereo image pairs. In the current setup, a section of the needle is occluded, however, in the images due to the presence of the needle driver. To overcome the occlusion and to estimate the new needle pose a discretization of the reconstructed needle and the needle defined by the optimum position is performed. Starting from the needle tip, points are sampled along the needle shape at distance equal to the arch length of 1 millimetre generating a set of equidistant 3D points, defined by N_{ide} for the ideal and N_{est} for the reconstructed needle, respectively. Finally, a rigid transformation that best maps the two set of points N_{ide} and N_{est}, i.e. the new needle pose, is calculated using singular value decomposition (SVD).

D. Task execution

With the learnt sewing movements, the robot is able to perform sewing in a continues manner. The whole sewing process is described as below:

1) Needle driver holding the end point of the needle
2) Vision system detects the needle pose relative to the needle driver
3) New robot trajectory is generated according to the needle pose
4) Needle driver approaching mandrel
5) Needle piercing into the fabric until the tip piercing out of fabric
6) Needle driver releasing the end point of the needle, approaching the needle tip
7) Needle driver griping the needle tip and pulling out the needle out of fabric
8) Needle driver bringing the needle to the second needle driver
9) The second needle driver griping the middle of the needle
10) The first needle driver griping the end point of the needle
11) The robot holding the mandrel moves to the next stitch position

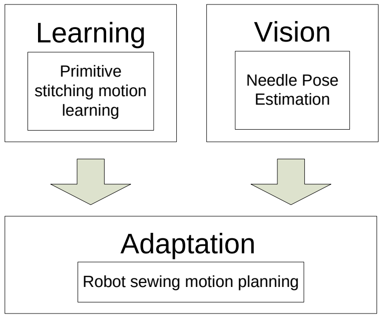

Fig. 5: System overview of stent graft sewing system. The robot is programmed by demonstrations. During task execution, the vision system estimate the needle pose and hence compute an adaptive trajectory for the sewing movements

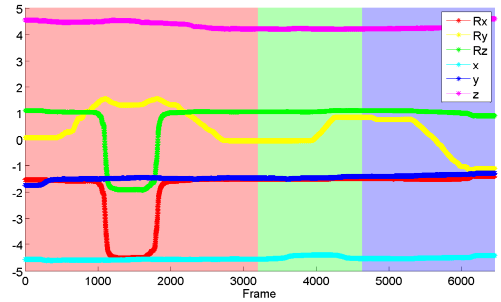

Fig. 6: Segmentation result of human demonstration. The red, green and blue patches label the three segments of the motion

12) The first needle driver move back to the starting position and ready to start the next cycle

During this process, the interactions between the needle and the driver is very possible to change their relative pose, which is monitored by the vision system. Once we detect the relative pose is changed, we recompute the robot piercing trajectory in order to adapt to the changes. The new robot trajectory is computed as:

$$T^{R}_{new} = T^{R}_{learnt} \dot{T}^{EE}_{optimumneedle} \dot{T}^{EE}_{currentneedle} \tag{8}$$

where T^{R}_{new}, T^{R}_{learnt} are the new robot end effector trajectory, the learnt trajectory and $T^{EE}_{optimumneedle}$, $T^{EE}_{currentneedle}$ the optimum needle pose, the current needle pose in the end effector frame. As mentioned in the previous two sections, the T^{R}_{learnt} is learnt from human demonstration of sewing, the $T^{EE}_{currentneedle}$ is detected by the vision system and the $T^{EE}_{optimumneedle}$ is the optimum pose we place the needle in initially. By correctly detecting the current needle pose, we are able to generate adaptive movements to sew stable stitches. In the next section, we detail the experiments we carry out with this system and present our results.

III. Experiments

A. System setup

A system with two articulated KUKA Lightweight-4 robots is built (Figure 1): one robot is mounted with a motorized needle driver holding a curved needle while the second robot holds a mandrel with a stent graft. The mandrel, shown in Fig 2, is a cylinder with grooves for fixing the stent and is characterized by the presence of slots to allow the sewing. The stereo system is consisted of two Logitech C930E cameras. Calibration of the stereo system is performed by using the OpenCV library. The camera frame is registered to the robot frame by hand-eye calibration. By knowing the relative position between the robot and the needle driver, and the transformation between the robot frame and the camera given by the hand-eye calibration, the needle driver pose in the camera frame can be computed. The needle is initially grip at the very end of the needle driver and we assume that only small displacement of the needle pose will occur during the sewing task. The needle driver tip position is hence used as a prior of the needle position.

B. Learning

For teaching robot the sewing task, we carry out four demonstrations. All demonstrations starts from the same position and sew the same slot on the mandrel. To control the quality of the stitches, across all demonstrations the needle pierces in at the same location and pierces out at the same location. At the beginning of each demonstration, the needle is placed at the same place and normal to the needle driver.

The demonstrations are segmented into three primitive movements, according to the needle drive open and close even. Figure 6 shows one segmentation results. Figure 7 shows the demonstrated needle driver trajectories in 3D.

GMM is used to learn model for each phase. Figure 8 shows a 2D projection of the build model of each phase. It can be seen from the model that the three phases have different characteristics. Phase one has small variance from the beginning to the end, as all the movements start from the same point and pierce into the same location. The piercing movements are the same in order to produce similar stitches. Phase two has larger variance compare to phase one, as the needle is detached with the robot and the robot movement has less constraints. Phase three has small variance at the beginning, when the robot needs to pull out the needle from the same location, and has large variance once the needle is pulled out from the fabric. These show that the GMM can effectively capture the constraints at each phase and hence generate proper trajectories for the robot to complete the task.

C. Task execution

Before starting replay the learned trajectory, a needle pose detection is performed using the stereo cameras and the transformation between the new needle pose and the optimal needle pose is calculated. Then a new needle driver trajectory is generated according to the transformation. If the needle pose is different with respect to the one presented during the demonstration, then the robot needs to adapt to a new pose in order to pierce the fabric in the same way it did during the demonstration.

In order to test our system to cope with variations on the needle pose, different needle poses are defined with respect to the one used during the demonstration, i.e. the optimal needle pose. A set of seven poses are defined where the variations ranges between 10mm translation along the

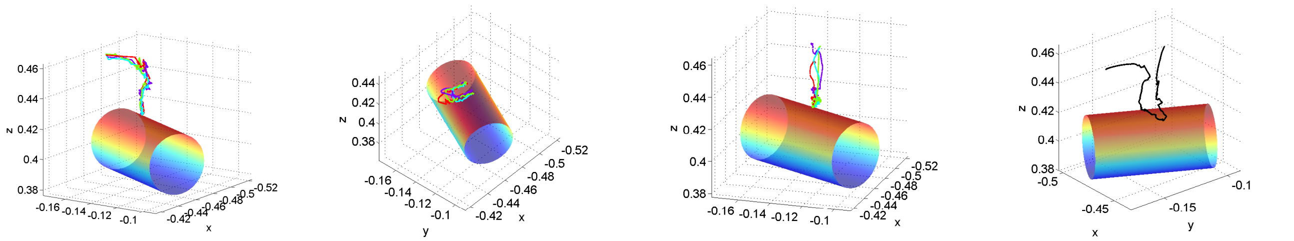

(a) Demonstrations of phase 1 (b) Demonstrations of phase 2 (c) Demonstrations of phase 3 (d) Learnt trajectory of phase 1,2 and 3

Fig. 7: Needle driver trajectories of human demonstrations and the learnt result. Each color represents one demonstration. The cylinder represents the mandrel

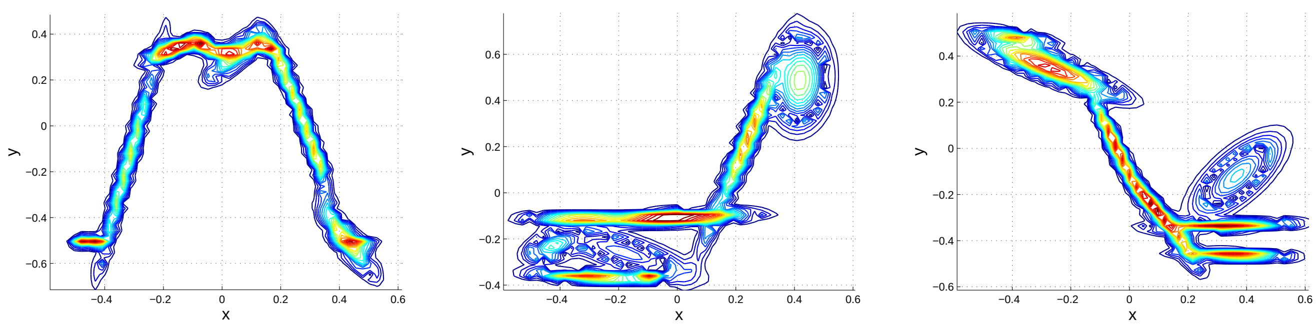

(a) Phase 1 (b) Phase 2 (c) Phase 3

Fig. 8: 2D representation of the learnt models of different phases.

grasper, and 20 rotation respectively around the point being grasped. During the experiment, the system successfully coped with the needle pose variations six times and failed once, resulting in a 86% of successful rate. The error in the piercing positioning into the fabric was less than 2mm. The only failure occurred was caused by the joint limits of the robot, which were reached during the experiment involving a rotation of -20 the needle. For the purpose of effective using joint range, a weighted Jacobian matrix is used with punishment on the most saturated joints. Figure **??** shows the results of the experiment for five different poses included the optimal needle pose.

Needle regripping is another important procedure for closing one stitching sequence. In order to sew continuously, the needle gripped by its tip point needs to be passed to another fixed needle driver. For this purpose, we demonstrate 3 trajectories for passing the needle between two needle drivers. At the start of the demonstration, the needle driver takes the needle and feeds it into another fixed needle driver. The fixed needle driver grip the middle point of the needle so that the moving needle driver can grip the needle back at its end point. Afterwards, the moving needle driver goes to the initial sewing position and the needle detection is performed for a new sewing cycle. Figure 10 shows the result of successful execution of the learned trajectory for the needle regripping task.

D. Vision for needle pose estimation

Extensive evaluation of the needle reconstruction algorithm is performed by estimating the 3D needle reconstruction error. This metric measures the distance between the reconstructed 3D shape and the ground truth shape of the needle. The ground truth is generated by segmenting manually the positions of the needle in each stereo image which are then used to find the ground truth 3D needle shape by triangulation. The 3D needle reconstruction error, i.e. $Dist(N_{gt}, N_{est})$, between the estimated needle, N_{est}, with respect to the ground truth shape, N_{gt}, is defined as:

$$Dist(N_{gt}, N_{est}) = \frac{1}{w+f}\left(\sum_{i=1}^{w} d_{min}(N_{gt}(i), N_{est}) + \sum_{j=1}^{f} d_{min}(N_{est}(j), N_{gt})\right) \tag{9}$$

where w and f are the cardinality of the set of points of N_{gt} and N_{est}, respectively, and $d_{min}(N_{gt}(i), N_{est})$ is the Euclidean distance between the i^{th} point of N_{gt} to the closest point on N_{est}. The distance $Dist$ is also presented in [19]. The mean and standard deviation of the 3D needle reconstruction error for the experiment involving seven different needle poses is 0.512 ± 0.097 millimetres. Thus, the needle reconstruction reaches sub-millimetres accuracy allowing a robust needle pose estimations which intrinsically depend on the needle reconstruction.

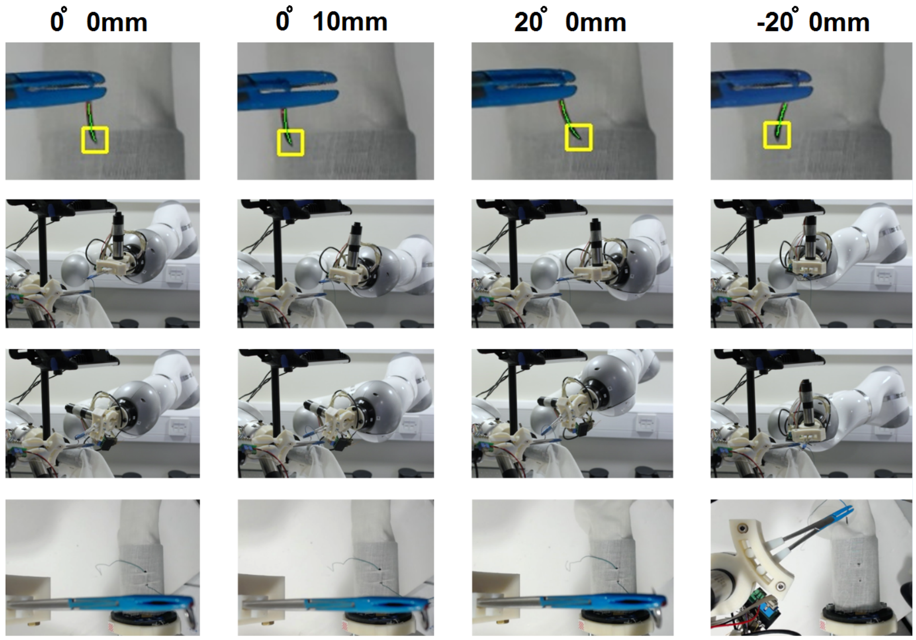

Fig. 9: Qualitative results of the task execution are shown for five different initial needle positions. Detection of the needle in the images is reported in the first row, while the robot adaptation during the task execution is shown in the second and third row. The end of the task is in the last row.

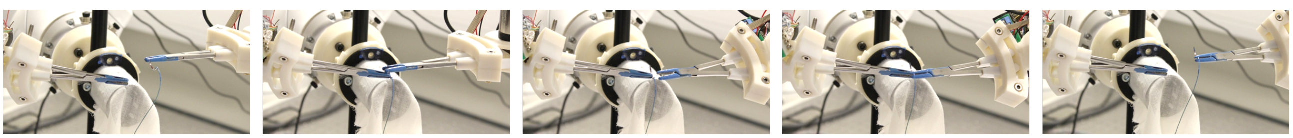

Fig. 10: Sequence of images that shows the automated needle regripping between the two needle driver.

IV. Conclusion

In this paper a robotic system for sewing a stent graft is presented. We successfully teach the robot to sew with a curved needle as well as adapt to needle posture changes using a vision guidance system (needle posture re-detection). We analyse the robustness of our method quantitatively by two experiments: fabric piercing and needle regripping, which are the two critical parts for completing one sewing stitch. We show that our system is able to accomplish the sewing task effectively. Our vision system reconstructs the needle shape with sub-millimetres accuracy, and hence is able to guide robustly the robot to sew. The successful rate of our system is over 86%. The failure case is due to the limited workspace caused by the robot joint limit. This problem can be leased by optimizing the task priority in the null space [**?**].

In this study, we use a single robot to manipulate the needle. The successful rate can be improved by using a second robot to cooperate the manipulation. This would make the tasks of both robot easier and also optimize each robots joint utilization. Our current system works as an open-loop manner for the needle adaptation part. Tracking the needle in real-time and implementing visual servoing algorithm is desired to increase the sewing accuracy. Further, the sewing presented is conducted in traditional way with needle drivers, in the future, customized sewing device will be designed by us to replace the needle holder to drive the needle performing fine movement.

The system presented in this paper is a primary and promising study of robot hand sewing. Applications of the presented system and method are not limited only for stent graft sewing; it is also a promising technique for automating robotic suturing.

References

[1] Donald J Berndt and James Clifford. Using dynamic time warping to find patterns in time series. In *KDD Workshop*, volume 10, pages 359–370. Seattle, WA, 1994.

[2] D.A. Cohn, Z. Ghahramani, and M.I. Jordan. Active learning with statistical models. *Journal of Artificial Intelligence Research*, 4:129–145, 1996.

[3] Srikrishna Iyer, Thomas Looi, and James Drake. A single arm, single camera system for automated suturing. In *Robotics and Automation (ICRA), 2013 IEEE International Conference on*, pages 239–244. IEEE, 2013.

[4] Russell C Jackson and M Cenk Cavusoglu. Needle path planning for autonomous robotic surgical suturing. In *Robotics and Automation (ICRA), 2013 IEEE International Conference on*, pages 1669–1675. IEEE, 2013.

[5] Ankur Kapoor and Russell H Taylor. A constrained optimization approach to virtual fixtures for multi-handed tasks. In *Robotics and Automation, 2008. ICRA 2008. IEEE International Conference on*, pages 3401–3406. IEEE, 2008.

[6] Panagiotis Koustoumpardis, Nikos Aspragathos, and Paraskevi Zacharia. *Intelligent robotic handling of fabrics towards sewing*. INTECH Open Access Publisher, 2006.

[7] Makoto Kudo, Yasuo Nasu, Kazuhisa Mitobe, and Branislav Borovac. Multi-arm robot control system for manipulation of flexible materials in sewing operation. *Mechatronics*, 10(3):371–402, 2000.

[8] Simon Leonard, Kyle L Wu, Yonjae Kim, Alexandra Krieger, and Peter CW Kim. Smart tissue anastomosis robot (star): A vision-guided robotics system for laparoscopic suturing. *Biomedical Engineering, IEEE Transactions on*, 61(4):1305–1317, 2014.

[9] Diego Lo, Paulo RS Mendonça, Andy Hopper, et al. Trip: A low-cost vision-based location system for ubiquitous computing. *Personal and Ubiquitous Computing*, 6(3):206–219, 2002.

[10] Hermann Mayer, Faustino Gomez, Daan Wierstra, Istvan Nagy, Alois Knoll, and Jürgen Schmidhuber. A system for robotic heart surgery that learns to tie knots using recurrent neural networks. *Advanced Robotics*, 22(13-14):1521–1537, 2008.

[11] Florent Nageotte, Philippe Zanne, Michel De Mathelin, and Christophe Doignon. A circular needle path planning method for suturing in laparoscopic surgery. In *Robotics and Automation, 2005. ICRA 2005. Proceedings of the 2005 IEEE International Conference on*, pages 514–519. IEEE, 2005.

[12] Nicolas Padoy and Gregory D Hager. Human-machine collaborative surgery using learned models. In *Robotics and Automation (ICRA), 2011 IEEE International Conference on*, pages 5285–5292. IEEE, 2011.

[13] Hedyeh Rafii-Tari, Alessandro Vandini, Lin Zhang, Archie Hughes-Hallett, and Guang-Zhong Yang. Vision-guided learning by demonstration for adaptive surgical robot control. In *Hamlyn Symposium*, pages 39–40, 2015.

[14] Johannes Schrimpf, Magnus Bjerkeng, and Geir Mathisen. Velocity coordination and corner matching in a multi-robot sewing cell. In *Intelligent Robots and Systems (IROS 2014), 2014 IEEE/RSJ International Conference on*, pages 4476–4481. IEEE, 2014.

[15] Johannes Schrimpf and Lars Erik Wetterwald. Experiments towards automated sewing with a multi-robot system. In *Robotics and Automation (ICRA), 2012 IEEE International Conference on*, pages 5258–5263. IEEE, 2012.

[16] Johannes Schrimpf, Lars Erik Wetterwald, and Morten Lind. Real-time system integration in a multi-robot sewing cell. In *Intelligent Robots and Systems (IROS), 2012 IEEE/RSJ International Conference on*, pages 2724–2729. IEEE, 2012.

[17] Christoph Staub, Takayuki Osa, Alois Knoll, and Robert Bauernschmitt. Automation of tissue piercing using circular needles and vision guidance for computer aided laparoscopic surgery. In *Robotics and Automation (ICRA), 2010 IEEE International Conference on*, pages 4585–4590. IEEE, 2010.

[18] Jur Van Den Berg, Stephen Miller, Daniel Duckworth, Humphrey Hu, Andrew Wan, Xiao-Yu Fu, Ken Goldberg, and Pieter Abbeel. Superhuman performance of surgical tasks by robots using iterative learning from human-guided demonstrations. In *Robotics and Automation (ICRA), 2010 IEEE International Conference on*, pages 2074–2081. IEEE, 2010.

[19] T. van Walsum, S. A M Baert, and W.J. Niessen. Guide wire reconstruction and visualization in 3DRA using monoplane fluoroscopic imaging. *IEEE Trans. Med. Imag.*, 24(5):612–623, 2005.